

Structural refinements and ab-initio calculations for Au₃Zr phase

P. PALADE*, C. CIOBANU^a

National Institute of Materials Physics, Atomistilor 105 bis, 077125 Magurele, Romania

^aPolitehnica University of Bucharest, 011061 Gheorghe Polizu 1-7, Bucharest

Au₃Zr intermetallic phase was obtained as pure phase by melt spinning technique. The sample with the same composition obtained by powder metallurgy exhibits some Au₄Zr impurity. Rietveld refinements of the X-Ray data were done to obtain the unit cell parameters and atom positions inside the unit cell. Geometry optimizations for the atom positions inside the unit cell were performed by using ab-initio band structure calculations. The calculated values agree well with the ones obtained by Rietveld refinements of the diffraction data. The electronic mechanisms are explained on the basis of the projected densities of states to atom sites.

(Received January 13, 2010; accepted February 02, 2010)

Keywords: Au₃Zr intermetallic, Melt spinning, Rietveld refinements, Electronic properties

1. Introduction

Au-Zr intermetallic compounds exhibit interesting applications acting as catalysts for CO oxidation [1-2]. A good description of Au-Zr phase diagram, at least concerning the Au-rich and Zr-rich part, was assessed by Massalski et al. [3]. A recent update of the Au-Zr phase diagram was given by Lommel-Tafin et co-workers [4-5]. They found new phases for the compositions of the middle of phase diagram: Zr₃Au₂ and AuZr. The intermetallics with Au/Zr stoichiometry close to 1:1 are very easily oxidizing and the product results obtained after exothermic reactions are Au and ZrO₂ [5]. From the practical point of view this is an easy and cheap way to obtain very fine Au particles dispersed on ZrO₂ support, with good catalytic effect [6]. Au₃Zr belongs to Cu₃Sb prototype (Pm3n group) [4]. There are two non-equivalent Au Wyckoff positions with 2b and 4f symmetry and one Zr position with 2a symmetry. Reference [4] and subsequent publications do not give the refined positions for these atoms.

Taking into account the potential applications of Au-Zr, in particular Au₃Zr, we studied deeply its structure. Firstly one searched for obtaining this compound as pure phase. This was not possible by arc melting and subsequent annealing. One had to use the melt spinning technique in order to get it. Rietveld refinements of the X-Ray diffraction data using Maud code [7] were performed. The refined atom positions obtained with Maud code were compared with the ones obtained by geometry optimizations using Wien2k code [8]. Moreover, we performed band structure calculations for Au₃Zr in order

to obtain the projected density of states to atom sites and to describe the electronic mechanisms which occur.

2. Experimental

Au and Zr foil (Alfa Aesar, 99.999%) were melted together under protective argon atmosphere (Ar 5.0) in the stoichiometric ratio (3:1) using an arc melting furnace. The melting procedure was repeated five times in order to ensure homogeneity. The sample was weighted before and after melting and the weight loss was less than 0.1 wt%. The as obtained sample was afterwards covered with tantalum foil, sealed under vacuum in quartz tube and annealed at 950 °C for 1 week. Another sample with similar composition was obtained using a commercially available Buehler melt spinner starting from the pre-melted material previously obtained by arc melting technique. The X-Ray data were obtained for both samples using a Bruker D8 Advance diffractometer with Cu K α radiation. Rietveld refinements were performed using MAUD [7].

3. Band structure calculations

In order to have a theoretical confirmation of the values obtained for the refined atomic positions of Au and Zr inside the Au₃Zr unit cell we performed band structure calculations using the WIEN2k program [8]. This code is based on LAPW [9] (Linear Augmented Plane waves method) and APW+lo [10] (Augmented plane waves plus local orbital) methods. The one-electron wave functions

are assumed to be combinations of radial functions multiplied by spherical harmonics inside the muffin-tin spheres and plane wave expansion between the spheres, in interstitial. The functions are matched in values and slopes at the spheres boundary. The valence charge density is computed from the eigenvectors, resulted after solving the secular equation of the crystal hamiltonian. The potential between the muffin-tin spheres is computed from the interstitial charge density and does not have shape approximation. The electronic valence charge and the potential are expanded in lattice harmonics inside the muffin-tin (MT) spheres and plane wave series in interstitial.

The electronic charge density was calculated in the frame of DFT theory, starting from Kohn-Sham equations [11] using the GGA approximation for the exchange correlation energy in the parameterization of Perdew [12]. The 4s and 4p Zr atomic states and 5p Au atomic states were analyzed like semi-core states and the corresponding electrons described by augmented plane wave functions and local orbitals [13]. The Au 6s, and Au 5d atomic states as well as Zr 4d and 5s atomic states were considered valence states characterized by augmented plane wave functions. All the other Zr and Au atomic states were treated as core states and calculated like atomic states under the effect of the crystal potential.

The core electrons were analysed in a fully relativistic way while the semi-core and valence electrons by scalar relativistic approach. The MT radii we used in the calculations were: $R_{MT}=2.5$ a.u. for Au and 2.4 a.u. for Zr (1 a.u. = 0.529177 Angstrom). A $(RK)_{max} = 8$ cut-off parameter was used, resulting in a basis set of about 200 plane waves per each non-equivalent atom inside the unit cell. The one-electron wave functions were expanded in radial functions series inside the MT spheres up to the orbital quantum number $l=10$. The electronic charge density and the potential were expanded into lattice harmonics inside the MT spheres up to the orbital quantum number $L=6$ both for Au and Zr. The electronic charge density and the potential were expanded into plane waves series in interstitial. The Fermi level was calculated by the modified tetrahedron method [14]. A “k mesh” in the irreducible wedge of the First Brillouin Zone (IZB) with 254 k points was used.

Very useful information about the electronic transfer processes between Au and Zr for the Au_3Zr compound was obtained from the site projected density of states inside the Au, respectively Zr MT sphere. According to LAPW (APW + lo) formalism the density of states can be decomposed in spherical harmonic contributions inside the MT spheres both to Au and Zr site.

4. Results and discussion

Fig. 1 shows the X-Ray diffraction pattern of Au_3Zr obtained by arc melting and subsequent annealing under vacuum. Besides the majority phase (Au_3Zr) it can be observed some small contribution of Au_4Zr . This is the

reason why to use the melt spinning technique in order to obtain a better phase purity.

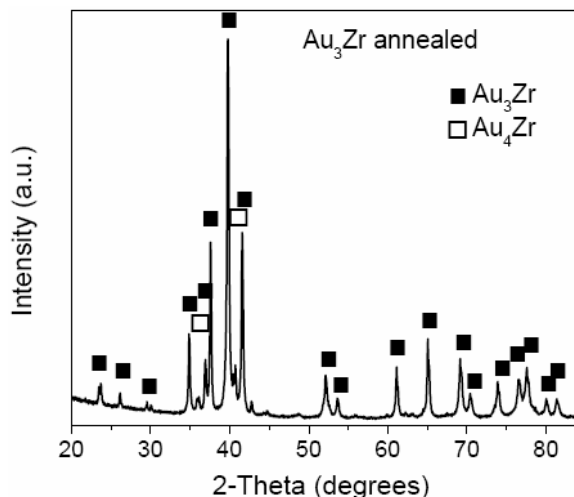


Fig. 1. X-Ray data of arc melted and subsequent annealed Au_3Zr .

Fig. 2 presents the X-ray data together with Rietveld refinements for melt spun Au_3Zr sample obtained using MAUD program. Au_3Zr was obtained as pure phase by this technique.

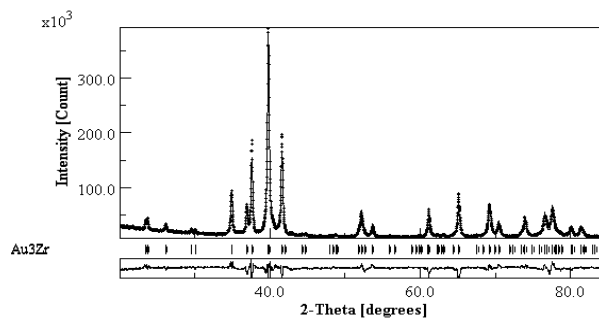


Fig. 2. Rietveld refinements of Au_3Zr sample obtained by melt spinning

The phase belongs to orthorhombic system, Pmmn group (No. 59). The refined lattice parameters obtained by Rietveld analysis are: $a = 0.60773(5)$ nm, $b = 0.48016(5)$ nm,

$c = 0.48867(5)$ nm.

Gold occupies two different Wyckoff positions inside the unit cell:

- (I) Au(2b) ($x=0.75(F); y=0.25(F); z=0.172(2)$),
 - (II) Au(4f) ($x=0.003(1); y=0.75(F); z=0.334(1)$),
- Zr is situated on (2a) Wyckoff position:
- (III) Zr(2a) ($x=0.25(F); y=0.25(F); z=0.173(2)$).

The refined atom positions without error bars are fixed by symmetry. F means fixed (non refining) Geometry optimizations for the atom positions have been performed using WIEN2k by moving the ions from the nodes of the unit cell in the direction of forces in such a way that both the forces acting on the ions and the total

energy per unit cell (ions and electrons) become minimum (forces to the ions decrease below 2 mRy/a.u.). The self-consistent calculations run until the forces vary less than 0.1 mRy/a.u. and the total energy less than 0.0001 eV for three consecutive iterations (the convergence criteria). For each step of structural optimization one needs a new self consistent calculation of the electronic charge and in consequence they are highly time consuming. The Wyckoff positions correspond to the space group previously given in literature [3-4], but the positions not fixed by symmetry have variational freedom during optimizations. The atom positions obtained from calculations are very close to the same parameters resulted from the refinements of the X-Ray data. The optimized atom positions are:

- (I) Au(2b) ($x=0.75$ (F); $y=0.25$ (F); $z=0.174$),
- (II) Au(4f) ($x=0.005$; $y=0.75$ (F); $z=0.331$),
- (III) Zr(2a) ($x=0.25$ (F); $y=0.25$ (F); $z=0.163$).

Total and site projected densities of states to Au and Zr sites are presented in Fig. 3. For Au were taken into account both non-equivalent positions. It can be observed that Au contribution is dominant in the range $-8 \div -3$ eV below Fermi energy (in all figures at 0 eV) and Zr is evident above Fermi energy ($1 \div 4$ eV). Au(2b) and Au(4f) contributions to the total density of states are similar, of course Au(4f) is about twice more important than Au(2b) according to the site occupancies. However it is evident a difference in the shape of their DOS at $(-5 \div -4$ eV) interval due to a different distortion of the local environment. There is a nonzero (flat) density of states to the Fermi energy proving a metallic behaviour of the intermetallic. Zr contribution above Fermi energy has a double peak shape due to ($d_{eg} - t_{2g}$) splitting.

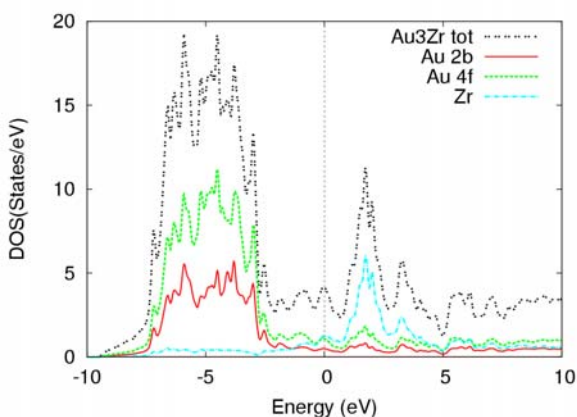


Fig. 3. Total and site projected densities of states for Au₃Zr.

Figs. 4 and 5 show the symmetry decomposed density of states to Au(2b) and Zr sites respectively.

It is clear that the bands down to -10 eV below Fermi energy have Au d dominant character (provided by Au 5d atomic states) and the bands up to 10 eV above Fermi energy have Zr d dominant character. The s and p contributions in both regions are spread in energy, only s contribution to Au site at about -7.5 eV being more

evident. The bands around this certain energy are hybrid bands with mixed s-d character. There is not a proof of mixing Au 5d and Zr 4d atomic states to create hybrid bands with bonding and anti-bonding states.

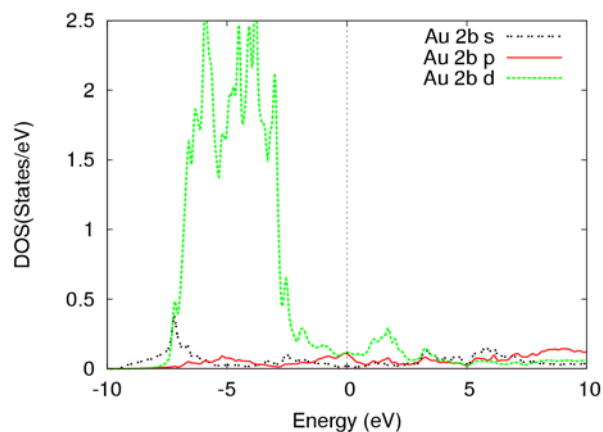


Fig. 4. Symmetry decomposed densities of states to Au(2b) site.

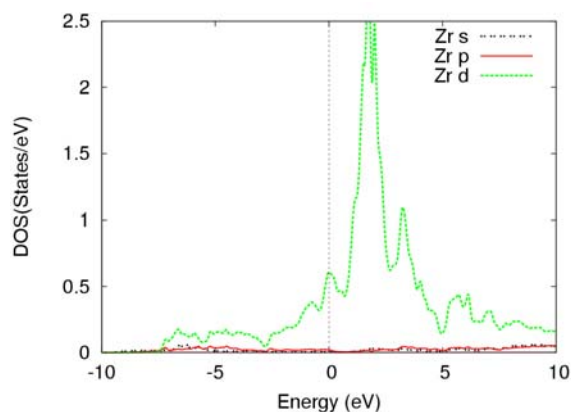


Fig. 5. Symmetry decomposed densities of states to Zr site.

Very probable the small d contribution at about 1.5 eV to Au site is caused by “tailing” phenomena caused by Zr d states. In both cases (above and below Fermi energy) the bands keep mainly the Au 5d and Zr 4d atomic character. The hybridization does not create evident bonding and anti-bonding bands by mixing the atomic contributions of Au and Zr.

5. Conclusions

Au₃Zr phase can be obtained as pure phase only by melt spinning technique. The sample with the same composition obtained by powder metallurgy presents also a small amount of Au₄Zr. Rietveld refinements of the experimental X-Ray data and geometry optimization calculations based on ab-initio band structure methods were used to get the atom positions inside the Au₃Zr unit cell. The values obtained by the two different of the methods are in very good agreement. The density of states

calculations proved a metallic behaviour of Au₃Zr in agreement with the experimental evidence. The bands down to 10 eV below Fermi energy have mainly Au d contribution but Zr d DOS is dominant for the bands up to 10 eV above Fermi energy. In both cases the bands have mainly atomic character and there is no evidence of mixing between Au 5d and Zr 4d atomic states.

Acknowledgements

The support of the Romanian Ministry of Education and Research through the project IDEI 1382 / 2008 "Non-usual electronic mechanisms in intermetallics: from electron pumping to selective adsorption processes concerning the surfaces" – is strongly acknowledged. C. Ciobanu acknowledges the financial support of the POSDRU - ID7713 doctoral fellowship.

References

- [1] J. Ch. Valmalette, M. Isa, M. Passard, M. Lomello-Tafin, *Chem. Mater.*, **14**, 2048 (2002).
- [2] N. Endo, S. Kameoka, A.P. Tsai, Z. Lingling, T. Hirata, C. Nishimura, *J. Alloys. Compd.* (2009), doi:10.1016/j.jallcom.2009.06.032
- [3] T. B. Massalski, H. Okamoto, J. R. Abriata, *Bull. of Alloy Phase Diagrams* **6**, 519 (1985).
- [4] M. Lomello-Tafin, R. Galez, J. C. Gachon, R. Feschotte, J. L. Jorda, *J. Alloys Compd.* **257**, 215 (1997).
- [5] M. Lomello-Tafin, P. Galez, P. Feschotte, J. J. Kuntz, J. L. Jorda, J. C. Gachon, *J. Alloys Compd.* **267**, 142 (1998).
- [6] M. Lomello-Tafin, A. A. Chaou, F. Morfin, V. Caps, J.-L. Rousset, *Chem. Commun.* **3**, 388 (2005).
- [7] L. Lutterotti, P. Scardi, P. Maistrelli, *J. Appl. Crystallogr.* **25**(3), 459 (1992).
- [8] P. Blaha, K. Schwarz, G. K. H. Madsen, D. Kvasnicka, J. Luitz, 2001 WIEN2k, An Augmented Plane Wave + Local Orbitals Program for Calculating Crystal Properties (Schwarz K, Technische Universität Wien, Austria) ISBN 3-9501031-1-2.
- [9] O. K. Andersen, *Solid State Commun.* **13**, 133 (1973).
- [10] G. K. H. Madsen, P. Blaha, K. Schwarz, E. Sjöstedt, L. Nordström, *Phys. Rev. B* **64**, 195134 (2001).
- [11] W. Kohn, L. J. Sham, *Phys. Rev.* **140**, A1133 (1965).
- [12] J. P. Perdew, K. Burke, M. Ernzerhof, *Phys. Rev. Lett.* **77**, 3865 (1996).
- [13] D. J. Singh, *Planewaves, Pseudopotentials and the LAPW Method*, Kluwer Academic Publishers, Dordrecht, 115, 1994.
- [14] P. E. Blöchl, O. Jepsen, O. K. Andersen, *Phys. Rev. B* **49**, 16223 (1994).

*Corresponding author: palade@infim.ro